Analysis of the Charge Controlled Inductor Current Sensing Peak-Power-Tracking Solar Array Regulator

K.S. Lee, Y.J. Cho and B.H. Cho
School of Electrical Engineering Seoul National University
San 56-1 ShinLim-dong KwanAk-Ku Seoul Korea
Phone + 82-2-880-7260, Fax + 82-2-878-1452
e-mail: idjd@plaza1.snu.ac.kr

ABSTRACT – The peak-power-tracking solar array regulator sensing the inductor current is proposed. Since it uses the inductor current as the solar array output power information, the PPT control scheme can be greatly simplified. The charge controlled two-loop scheme is presented to improve the dynamics due to the inductor current sensing. The comparison between the single-voltage loop controlled system and the two-loop controlled system employing the charge control is presented. This paper also contains the simulation results of that comparison.

1. INTRODUCTION

For a low-earth-orbit (LEO) spacecraft power system, a solar array regulator (SAR) processes the solar array power to change the battery and to supply the load power during the sunlight period. The SAR operates mainly in two modes; the peak power tracking (PPT) mode and the current regulation (CR) mode depending on the status of the battery and load power demand.

As shown in Figure 1, the output characteristics of the solar array is highly nonlinear and it's output power depends on the operating point which is set by the SAR.

Figure2 illustrates a series SAR system widely used in a low-earth-orbit spacecraft power system in the PPT mode.

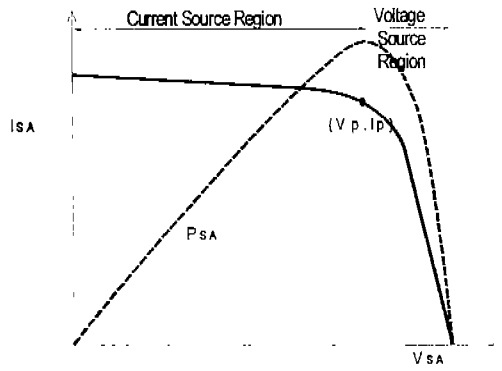

Figure 1. The nonlinear output characteristic of the solar array

The inner voltage loop regulates the solar array output voltage to the reference value from the PPT controller. The PPT controller calculates the solar array power by multiplying the sensed solar array voltage and current. From this information, the PPT controller tracks the solar array maximum power point by changing the reference value of the voltage controller. Various algorithms including digital algorithms can be used to track the maximum power point. [1,7]

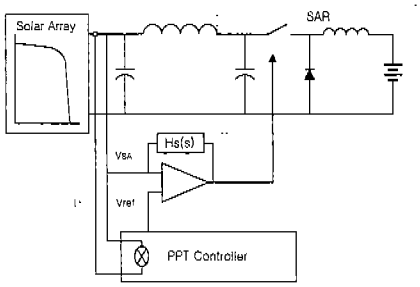

Figure 2. The Conventional series PPT system

Because the DC value of the inductor current in the SAR is proportional to the output power of the solar array, this inductor current information can be used in the PPT system instead of the solar array power. Furthermore this system greatly simplifies the PPT scheme especially for an analog PPT scheme because the multiplying operation in the PPT controller is not necessary. Figure 3 is the scheme of this system.

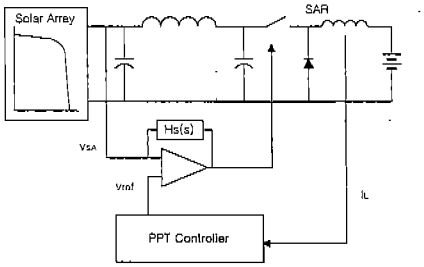

Figure 3. The inductor current sensing system (with single voltage loop)

The main difference between the two systems is that the stability of the PPT loop in the conventional system depends on the dynamics of the solar array voltage, while the inductor current sensing system depends on the inductor current in the SAR.

To improve the dynamics of the inductor current, the SAR employing the charge control is proposed as in Figure 4. In this system, the time average value of the switch current is cooperated into the inner loop operation.

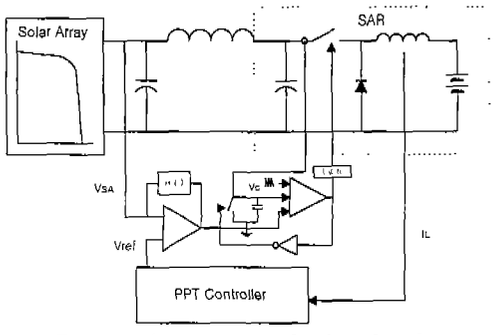

Figure 4. Proposed system employing the charge control scheme

2. SYSTEM DESCRIPTION

System description

Figure 4 shows the proposed SAR employing the charge control scheme. As in the conventional PPT system in Figure 2, the Vref is compared with the solar array voltage to generate the control voltage, Vc. This control voltage is then compared with the amount of charge in the switch of the PWM converter to control the duty ratio of the switch. The time average of the amount of charge per switching cycle is in fact the solar array current. Thus the solar array current information is feedback to control the duty ratio and this indirectly regulates the inductor current. As discussed in [2], the amount of the current loop gain for each loop varies depending on the dynamic resistance of the solar array output, r_s. Using this fact, the amount of feedback actions between the voltage loop and current loop can be optimally designed such that the current loop improves the dynamics of the inductor current.

Basic operation of the charge Control

The active switch in the power stage turns on at the beginning of each cycle, and the switch current is integrated by capacitor (Ct) to get total charge. When the voltage across Ct reaches the control voltage (Vc), the switch turns off, and the capacitor Ct is discharged before the next cycle starts. In this method, the total charge of the switch in one cycle - the average value of the switch, is controlled. The average switch current is the solar array output current, so solar array output current is controlled by the charge current loop. The voltage across the Ct is

$$V_t = \frac{1}{C_t}\int_0^{dTs} i_L(t)dt = \frac{Ts}{C_t} i_{SWA} \qquad (1)$$

where, Ts : Switching period
i_{SWA} : Average switch current

3. SMALL SIGNAL ANALYSIS

Inductor current sensing system (single loop)

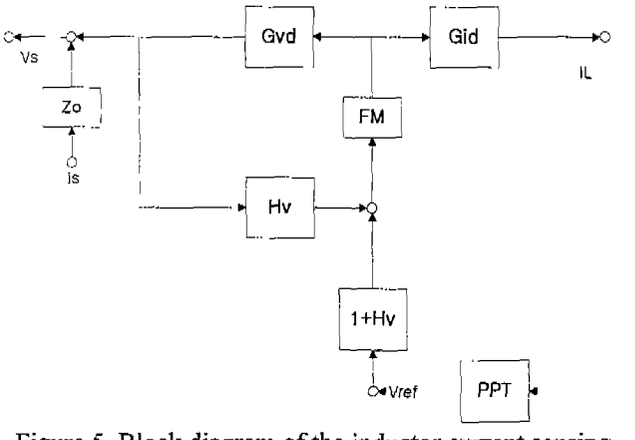

Figure 5. Block diagram of the inductor current sensing system (with single voltage loop)

Figure 5 shows the control block diagram of the system with the single voltage loop in Figure 3. It clearly shows the dynamics of the inductor current affects the stability of the system. Assuming the ESR of capacitor is very small, each blocks are derived as follows:

$$Gvd = -\frac{Vba}{D^2}\frac{(s/w_{z1}+1)(s/w_{z2}+1)}{s^2/w_o^2 + s/(Qw_o)+1} \qquad (2)$$

$$Gid = \frac{I_k}{D^2}\frac{(s/w_{z3}+1)}{s^2/w_o^2 + s/(Qw_o)+1} \qquad (3)$$

$$Zo = \frac{R_l}{D^2}\frac{(s/w_{z1}+1)(s/w_{z2}+1)}{s^2/w_o^2 + s/(Qw_o)+1} \qquad (4)$$

$$Hv = \frac{wi(s/w_1+1)(s/w_2+1)}{s(s/w_3+1)(s/w_4+1)} \qquad (5)$$

where, Fm : Control voltage to duty ratio

Vba : Battery voltage

D : Duty ratio

I_L : Average inductor current

V_s : Solar array output voltage

$$Q = \frac{1}{w_o[(R_c + R_l / D^2)C + \frac{L}{D^2 r_s}}$$

$$I_k = \frac{V_s}{r_s} - DI_L, \quad w_o = \frac{D}{\sqrt{LC}}$$

$$w_{z1} = \frac{1}{RcC}, \quad w_{z2} = \frac{R_l}{L}, w_{z3} = \frac{V_s C}{I_k}$$

The small signal transfer functions of the reference voltage to the inductor current and to the solar array output voltage are;

$$\frac{\hat{i}_L}{\hat{v}_{ref}} = \frac{FmGid}{1+Tv}(1+Hv) \qquad (6)$$

$$\frac{\hat{v}_s}{\hat{v}_{ref}} = \frac{FmGvd}{1+Tv}(1+Hv) \qquad (7)$$

where, $Tv = GvdFmHv$

Comparing (6) and (7) associating (2) and (3) there is no difference but zeros and gain. Because of having the same poles and Q, the inductor and the solar array output voltage dynamics have the same characteristic function. The difference in the location of zeros and DC gains makes them have different dynamics.

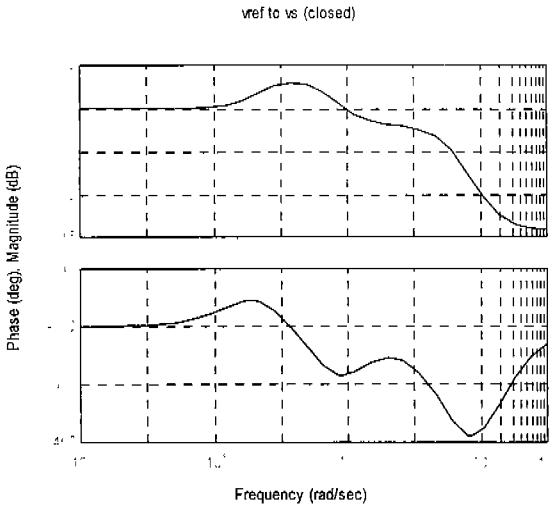

Figure 6. Bode plot of the reference voltage to the solar array output voltage (single loop system)

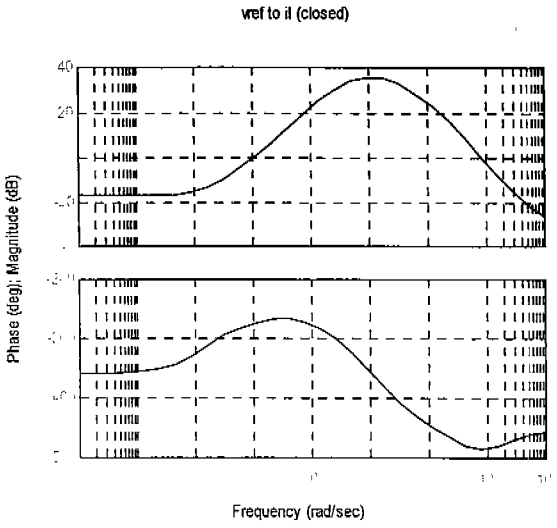

Figure 7. Bode plot of the reference voltage to the inductor current (single loop system)

Figure 6 and Figure 7 are the bode plots of (6) and (7) in the peak power point region. Comparing the DC gains, (6) has much smaller DC gain than that of (7), for I_k is very small around the peak power point region. Also the control to inductor current transfer function in (6) has a large peaking. It makes the dynamics of the inductor current be poorer than the solar array output voltage dynamics.

Figure 8 is the simulation results, showing the poor dynamics of the inductor current and as the result the PPT controller fails to track the maximum power point of the solar array.

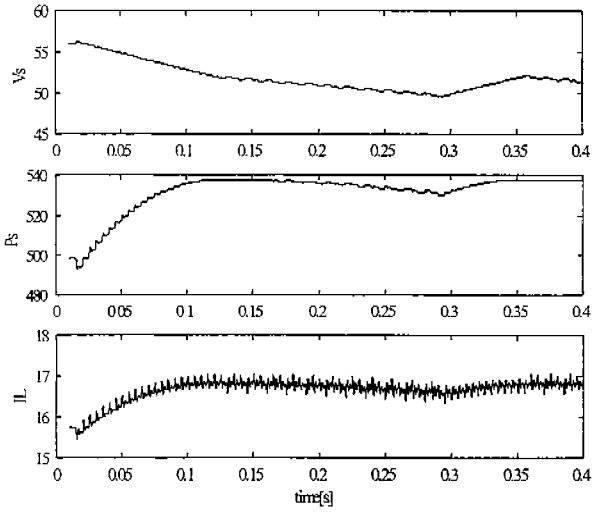

Figure 8. Simulation Results of the inductor current sensing system (with single voltage loop)
(The Peak Power point is about 52[V])

Inductor current sensing system (with the charge control)

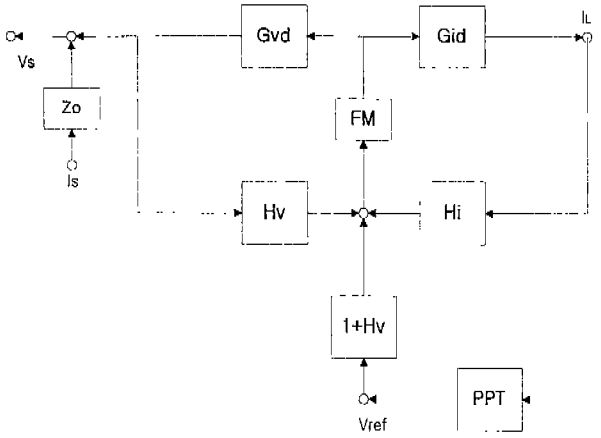

Figure 9. Block diagram of the proposed system employing the charge control

In order to improve the dynamic performance of the PPT scheme, the charge controlled two-loop system in figure 4 can be used. Figure 9 shows the control block diagram of the proposed system. Added blocks are derived as follows;

$$Fm = \frac{D}{(I_{LP} + SeCt)Ri} \tag{8}$$

$$Hi = RiHe \tag{9}$$

where, I_{LP} : Inductor peak current

Se : External ramp

Ts : Switching period

$$Ri = \frac{DTs}{C_t}, \quad He = 1 + \frac{s}{w_n Q_p} + \frac{s^2}{w_n^2}$$

$$w_n = \pi / Ts, \quad Q_p = -2/\pi$$

The small signal transfer functions of the reference voltage to the inductor current and to the solar array output voltage are;

$$\frac{\hat{i}_L}{\hat{v}_{ref}} = \frac{FmGid}{1 + Tv + Ti}(1 + Hv) \tag{10}$$

$$\frac{\hat{v}_s}{\hat{v}_{ref}} = \frac{FmGvd}{1 + Tv + Ti}(1 + Hv) \tag{11}$$

where, $Ti = FmGidHi$

Figure 10 and figure 11 are the bode plots of (10) and (11). *Ct*, *Se*, and *Hv* are designed as [2]. Because of *Ti* the peaking in the control to inductor current transfer function in figure 7 is reduced as shown in figure 11.

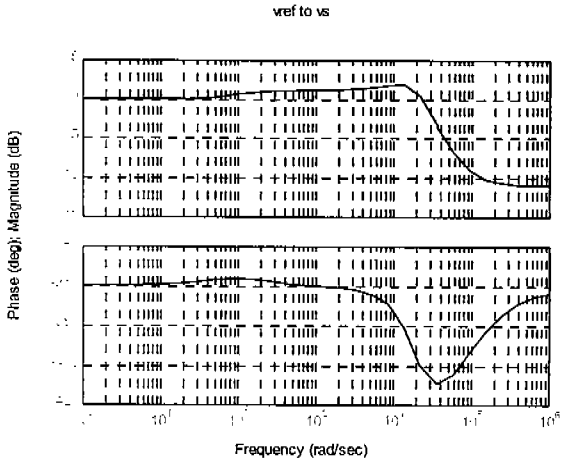

Figure 10. Bode plot of the reference voltage to the solar array output voltage (two loop system)

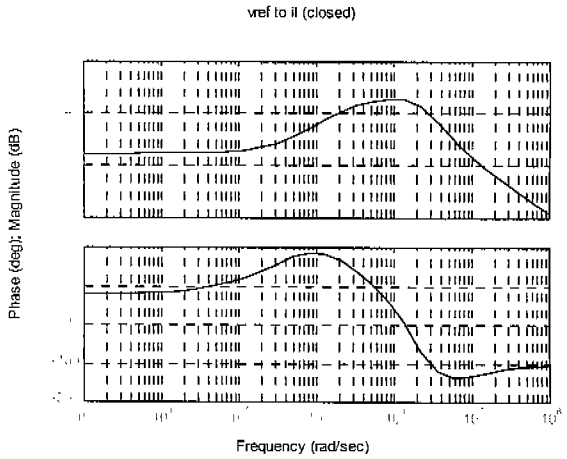

Figure 11. Bode plot of the reference voltage to the inductor current (two loop system)

Figure 12 shows the time domain simulation of the PPT.

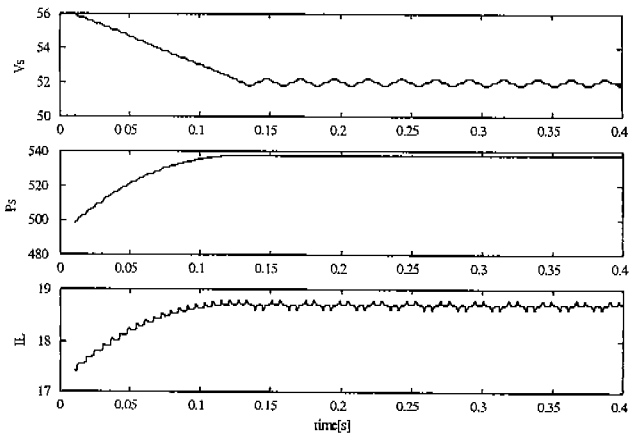

Figure 12. Simulation Results of the proposed system employing the charge control
(The Peak Power point is about 52[V])

It is important to note that the peak current mode control can not be used in this application. As stated earlier, the inductor current has the same profile as the solar array output power, considering the battery voltage is a fixed value. Thus, regulating the inductor current using the peak current mode control is not possible because the inductor current gain as the function of the solar array voltage changes its sign around the peak power point.

4. CONCLUSION

The peak-power-tracking system sensing the inductor current instead of the solar array output power is proposed. It has some advantages. The multiplier may not be used, the capacitor in front of the battery can be smaller, and because the inductor current is used as power information, PPT can track not the maximum solar array power but the maximum inductor current. To improve the dynamics, the current loop employing the charge control is added. The charge control scheme not only stabilize the system but also it can be utilized for the battery current regulation control loop.

5. REFERENCES

[1] Huynh, P., and B.H. Cho, "Analysis and Design of a Microprocessor-Controlled Peak-Power Tracking System," IECEC, 1992.

[2] Y.J. Cho, and B.H. Cho, "A Digital-Controlled Solar Array Regulator Employing the Charge Control," IECEC, 1997.

[3] Wei Tang, F.C. Lee, R.B. Ridley and I. Cohen, "Charge Control: modeling, analysis and design,:" in Proceedings of the IEEE Power Electron. Specialists Conf., 1992 pp.503-511

[4] R.B. Ridley, "A new continuous-time model for current mode control," IEEE Trans. Power Electron. Vol. 6, pp.271-280, April 1991

[5] V. Voperian, "The Charge-controlled PWM switch," PESC, 1996

[6] Steve J. Butler, Dan M. Sable, Fred C. Lee, and B.H. Cho, "Design of a Solar Array Simulator for the NASA EOS Testbed," IECEC, 1992

[7] J.R. Lee, B.H. Cho, "Modeling and Simulation of Spacecraft Power Systems," IEEE Transactions on AES, May 1988